International Dairy Journal 95 (2019) 18–24

Contents lists available at ScienceDirect

International Dairy Journal

journal homepage: www.elsevier.com/locate/idairyj

Behaviour of water in different types of goats' cheese

Jolanta Tomaszewska-Gras [a], Dorota Cais-Sokolińska [b, *], Paulina Bierzuńska [b], Łukasz K. Kaczyński [b], Katarzyna Walkowiak [c, d], Hanna M. Baranowska [c]

[a] Department of Food Quality Management, Faculty of Food Science and Nutrition, Poznań University of Life Sciences, ul. Wojska Polskiego 31, 60-624 Poznań, Poland
[b] Department of Dairy Products Quality, Faculty of Food Science and Nutrition, Poznań University of Life Sciences, ul. Wojska Polskiego 31, 60-624 Poznań, Poland
[c] Department of Physics and Biophysics, Faculty of Food Science and Nutrition, Poznań University of Life Sciences, ul. Wojska Polskiego 38/42, 60-637 Poznań, Poland
[d] Faculty of Technical Physics, Poznan University of Technology, ul. Piotrowo 3, 60-965 Poznań, Poland

ARTICLE INFO

Article history:
Received 29 October 2018
Received in revised form
14 January 2019
Accepted 25 February 2019
Available online 21 March 2019

ABSTRACT

Semi-hard, hard, and extra-hard goats' cheeses were analysed for water mobility by nuclear magnetic resonance relaxometry (NMR) and thermal properties by differential scanning calorimetry (DSC). In extra-hard cheese, the amount of bulk water as a proportion of the total water was the lowest, which indicated that the water was strongly entrapped in the proteolipidic network and bound by the water-soluble substances arising after increased proteolysis. The bulk water fraction is mainly a component of water-in-fat emulsions. The increase in H^+ ion concentration limits the mobility of bound water protons. Both the peak temperature and enthalpy progressively decreased with the lowering of moisture. A strong correlation was found between the NMR parameter T_1 (spin–lattice relaxation time) and the DSC freezable water content.

1. Introduction

Cheeses made from goats' milk have an established position among other cheeses (Haenlein, 2007), consumers appreciating their structure and aroma (Ryffel, Piccinali, & Butikofer, 2008). Knowledge of the relationships between cheese composition, e.g., casein–casein, casein–water, and casein–fat interactions, the state of the bulk water, or that bound to the casein matrix, the pH, and the extent of proteolysis, determines the final characteristics of the cheese (Arimi, Duggan, O'Sullivan, Lyng, & O'Riordan, 2008; Noronha, O'Riordan, & O'Sullivan, 2008b; Wang & Sun, 2002). During cheese ripening, the main components, i.e., fat, protein, and lactose, break down (Kirmaci, Hayaloglu, Özer, Atasoy, & Türkoglu, 2014; Michaelidou, Katsiari, Voutsinas, Polychroniadou, & Alichanidis, 2007; Shakeel-Ur Rehman et al., 2000). The secondary products produced from these degradation components are responsible for the structure of the cheese and its taste and smell, and thus its general desirability to consumers (Saurel, Pajonk, & Andrieu, 2004); protein degradation is essential for the proper development of flavour, body, and texture in all ripened cheeses.

The physical, biochemical, and microbiological changes taking place during the ripening are correlated with the quality, safety, and stability of the cheese. The persistence of desirable properties is closely associated with the presence and the state of the water in the product, so the analysis of water is important to determine the prevailing relationships of the water in cheese. It is important to determine the amount of free and bound water, as well as the behaviour of water molecules as the concentration of solute increases. Knowledge about water activity (a_w) and thermodynamic potential is the basis for predicting food durability and determining storage conditions. Water activity and sorption isotherms have been used as controlling factors for the ripening process of various cheeses (Saurel et al., 2004).

The value of a_w depends on the content of free water and the amount and type of soluble compounds. The process of cheese salting (NaCl) and the migration of salt from the boundary layers to the interior of the cheese plays a large role in cheese production technology (Pajonk, Saurel, Andrieu, Laurent, & Blanc, 2003; Saurel et al., 2004). The water activity is different in the case of whole

* Corresponding author. Tel.: +48 61 848 73 17.
E-mail address: cais@up.poznan.pl (D. Cais-Sokolińska).

https://doi.org/10.1016/j.idairyj.2019.02.015
0958-6946/

cheese salting, e.g., Cheddar, and that of other cheeses salted in brine. The NaCl concentrations affect a_w, which in turn controls the activity of proteolytic enzymes. During ripening, the proteolysis and peptidolysis occurring cause high molecular weight peptides to be degraded by bacterial enzymes into lower molecular weight peptides and free amino acids (Kirmaci et al., 2014). These processes affect the reduction in a_w. The intensity of these changes depends on the quantity and type of proteolytic microbial enzymes and the increased moisture content. However, effects on enzyme activity can be caused by the content of lactic acid, pH, temperature, oxidation-reduction potential, and the level of salts (Kanawjia, Rajesh, Sabikhi, & Singh, 1995; Moschopoulou, Anisa, Katsaros, Taoukis, & Moatsou, 2010).

For the evaluation of the availability of water in complex systems such as food, including cheese, nuclear magnetic resonance (NMR) and differential scanning calorimetry (DSC) are often used (Altan, Oztop, McCarthy, & McCarthy, 2011; Gliguem et al., 2009; Noronha, Duggan, Ziegler, O'Riordan, & O'Sullivan, 2008a). In NMR relaxometry, the measured relaxation times (the spin–lattice and transverse) are a measure of the mobility of water molecules. DSC has been proposed to detect the freezing and the melting temperatures of water in the emulsion by Clausse (2010). This technique permits the researcher to detect bulk and emulsified water by measuring the energy absorbed or released during phase transition. Both techniques allow the study of the behaviour of water in the cheese matrix, DSC at the global scale and NMR at the molecular level (Baranowska, Tomaszewska-Gras, Cais-Sokolińska, Bierzuńska, & Kaczyński, 2017; Cais-Sokolińska, Bierzuńska, Kaczyński, Baranowska, & Tomaszewska-Gras, 2018).

This research analysed the water behaviour and thermal properties of semi-hard, hard, and extra-hard goats' cheeses, differing in water content and with a constant ratio of fat to protein. There is no publication describing the behaviour of water in goats' cheeses with different contents of water-soluble extracts and free amino groups, which result from their ripening. This research allowed the entrapped water in the proteolipidic network to be evaluated, and the factors influencing the binding of water molecules to be found. The hypothesis was that the content of water in goats' cheeses with different degrees of ripening affects water distribution and mobility in cheese.

2. Materials and methods

2.1. Collection of the cheeses

Commercial goats' cheeses of various degrees of firmness and ripening were tested. The cheeses came from various producers from EU countries and were bought at local markets or directly from producers. These were cheeses made from unpasteurised milk. The cheese was stored at 4 ± 0.5 °C for no longer than 3 days. The percentage moisture on a fat-free basis (MFFB) was calculated using equation (1).

$$\mathrm{MFFB} = \frac{\text{Weight of moisture in the cheese}}{\text{Total weight of cheese} - \text{Weight of fat in the cheese}} \times 100 \quad (1)$$

The cheeses were divided into three groups according to Codex (2013): semi-hard (MFFB 49–56%), hard (MFFB 54–69%), and extra-hard (MFFB < 51%). Subsequently, cheeses were selected with a similar ($P > 0.05$) ratio of fat:protein (F:P) and similar ($P > 0.05$) fat in dry matter (FDM). Values of F:P = 1.2 and FDM = 50.7% turned out to be common. In this way, 20 cheeses were finally selected for the experiment. They were eight samples of semi-hard goats' cheese (SHG), seven hard (HG), and five extra-hard (EHG).

The cheeses were in different forms and had different coatings. Therefore, the inner layer of cheese closer to the geometric centre was taken for analysis. It was 2.5 cm away from the cheese surface – the outside layer of the cheese or cheese portion. Each sample was analysed three times.

2.2. Composition, pH, and proteolysis

The content of water, total nitrogen, and fat in the cheese was determined by standard methods (AOAC, 1995) described in detail by Cais-Sokolińska et al. (2018). Casein nitrogen was expressed as % of total nitrogen (N × 6.38). The pH of the cheese was measured with a CP-315 digital pH meter (Elmetron Co., Zabrze, Poland) equipped with a probe for solids used for measuring according to the manufacturer's recommendations.

The water-soluble extracts (WSE) were prepared according to the method of Kuchroo and Fox (1982), and their nitrogen content was determined using the macro-Kjeldahl method (Fox, 1989; Singh, Fox, Hojrup, & Healy, 1994). The concentrations of free amino groups in the WSE of cheeses were determined by the Cd-ninhydrin method of Folkertsma and Fox (1992).

2.3. Water activity

The water activity was determined with an AquaLab Series 4TE instrument (Decagon Devices Inc., Pullman, WI, USA) equipped with a thermostatic chamber controlled by means of measuring elements using the thermoelectric Peltier effect. The water activity was calculated (equation (2)) based on $p_f(T)$ – the value of the vapour pressure of the water that is in equilibrium with the sample maintained at a constant level during the measurement of temperature T, and $p_s(T)$ – the vapour pressure of saturated pure water at the same temperature T (Lewicki, 2004):

$$a_w = \frac{p_f(T)}{p_s(T)} \quad (2)$$

The accuracy of the determination was ±0.003 a_w and the measuring range 0.03–1.000 a_w. The determinations were carried out under conditions of thermodynamic equilibrium. The following salt solutions were used for reference: 0.5 M KCl of $a_w = 0.984$ (15 °C), 6 M NaCl of $a_w = 0.760$ (20 °C), 8.57 M LiCl of $a_w = 0.500$ (25 °C) and 13.41 M LiCl of $a_w = 0.250$ (25 °C). Samples of 15 mL were placed in a DE 501 measurement vessel (Decagon Devices Inc.) and tested at 15 °C.

2.4. Differential scanning calorimetry

A Perkin Elmer DSC 7 differential scanning calorimeter (Perkin Elmer, Norwalk, NJ, USA), equipped with an Intracooler II and running under Pyris software, was used to examine the water behaviour in cheese samples. Nitrogen (99.999% purity) was the purge gas. The DSC calorimeter was calibrated using indium (m.p. 156.6 °C, ΔHf = 28.45 J g^{-1}) and n-dodecane (m.p. −9.65 °C, ΔHf = 216.73 J g^{-1}). Samples of cheese (9–10 mg) were weighed into aluminium 20 μL pans (Perkin Elmer, No. 0219-0062), which were then hermetically sealed. The reference was an empty, hermetically sealed aluminium pan. The calibration of the calorimeter was controlled by melting capric acid (m.p. 31.6 °C). The sample pan was placed in the calorimeter at 5 °C, cooled at 5 °C min^{-1} to −40 °C, and then heated at 5 °C min^{-1} to 70 °C. Three replicates

were analysed for each sample. The reported data concerning ice melting included parameters of ice melting onset and peak temperatures (Ti_{onset}, Ti_{peak}) and the enthalpy of ice melting (ΔH_{ice}). The enthalpies were calculated per 1 g of water.

The percentage of freezable water (FW) in the water fraction was calculated as (equation (3)):

$$FW = \frac{\Delta H_{ice}}{\Delta H_{ref}} \cdot 100 \quad (3)$$

where ΔH_{ice} is the enthalpy of ice melting per unit mass of water contained in cheese (J g^{-1}) and ΔH_{ref} is the enthalpy of ice melting for samples of pure water, equal to 333.7 J g^{-1}.

2.5. NMR

Samples of 1.5 cm diameter and 1.2 cm height were placed in measuring test tubes and sealed using Parafilm. Measurements of the spin–lattice (T_1) and spin–spin (T_2) relaxation times were performed using a pulse NMR spectrometer operating at 30 MHz (WL Electronics, Poland). The inversion-recovery (180-TI-90) pulse sequence (Brosio & Gianferri, 2009) was applied for measurements of the T_1 relaxation times. The distances between impulses (TI) were changed within a range from 4 to 800 ms, and the repetition time was from 15 s. Each time, 32 FID signals and 119 points from each FID signal were collected. Calculations of the spin–lattice relaxation time values were performed with the assistance of the CracSpin program (Węglarz & Harańczyk, 2000), a program for calculating relaxation parameters from experimental data using a "spin grouping" approach. Marquardt's method of minimisation was applied for the fitting of multiexponential decays. The accuracy of the relaxation parameters was estimated using the standard deviation. The time changes of the current value of the FID signal amplitude in the applied frequency of impulses are described by the following formula (equation (4)):

$$M(t) = M_0\left(1 - 2\exp\left(\frac{-TI}{T_1}\right)\right) \quad (4)$$

where: M (t) – the actual magnetization value, M_0 – the equilibrium magnetization value, TI – the distance between impulses and T_1 – the spin–lattice relaxation time.

A monoexponential magnetization recovery was found, which means that the system relaxed with one T_1 spin–lattice relaxation time. Measurements of the T_2 spin–spin relaxation times were taken using the pulse train of the Carr–Purcell–Meiboom–Gill spin echoes (90-t-180_n) (Brosio & Gianferri, 2009). The distance (t) between 180 impulses amounted to 1 ms, while the repetition time was 15 s. The number of spin echoes (n) amounted to 50, and ten accumulation signals were employed. To calculate the spin–spin relaxation time values, the authors applied an adjustment of the values of the echo amplitudes to the formula (Baranowska, 2011; equation (5)):

$$M(t) = A\sum_{i=1}^{m} f_i \exp\left(\frac{-t}{T_{21}}\right) \quad (5)$$

where: M (t), echo amplitude; A, equilibrium amplitude; t, distance between 180 RF-pulses; f_i, fraction of protons relaxing with the T_{2i} spin–spin time; m, number of proton fractions.

The calculations were performed using the dedicated software by applying a non-linear least-squares algorithm, while the accuracy of the relaxation parameters was estimated with the standard deviation. The presence of two proton fractions was determined for all analysed systems.

2.6. Statistical evaluation

For the verification of statistical hypotheses, a level of significance of $\alpha = 0.05$ was adopted. The statistical calculations were carried out using Statistica data analysis software, version 10 (StatSoft, Tulsa, OK, USA).

3. Results and discussion

3.1. Water content and composition

According to the assumptions of the experiment, cheeses that did not differ with respect to their fat in dry matter (FDM = 50.7%) and their ratio of fat to protein (F:P = 1.2) were chosen for the study (Table 1). The highest level of moisture (46.40 g 100 g^{-1}) was found in the SHG cheese. Significantly less moisture was HG cheese (less by 19%) and EHG cheese (less by 36%). SHG cheeses contained the least fat and protein. The ratio of moisture to protein, calculated using the means of moisture and protein (M:P) was the highest in SHG (2.0). The lowest pH was measured in hard cheeses (pH 5.08) and the highest (pH 5.32) in EHG.

The basic chemical composition of the cheeses examined did not differ from those described in the literature. Fekadu et al. (2005) examined hard and semi-hard cheeses from goats' milk from various lactation periods. They showed that in hard cheese the fat content (g 100 g^{-1}) ranged from 26.42 to 29.45, the protein from 18.38 to 23.78. The moisture levels of these cheeses were in the range 36.30–39.74 g 100 g^{-1}. On the other hand, goats' semi-hard cheeses were moister, levels in the range 43.51–50.16 g 100 g^{-1}, with fat and protein lower than in hard cheeses; fat was in the range 19.83–23.45 g 100 g^{-1}, and the protein content was 15.19–22.17 g 100 g^{-1}. The moisture levels in the semi-hard goats' cheeses examined by Poveda, Sanchez-Palomo, Perez-Coello, and Cabezas (2008) were in the range 36.85–38.10 g 100 g^{-1}. The authors found that the pH of the samples was pH 4.85–5.57. Their cured cheese samples had a pH of 5.19 and 5.57, and the semi-cured samples a pH 4.85–5.30. In turn, Requena, De la Fuente, Fernandez de Palencia, Juârez, and Pelaez (1992), during their pilot study on semi-hard goats' milk cheese production, showed that the cheese pH was initially 5.47, after 30 days of ripening the pH was 5.34, but after 60 days it was close to the initial pH at 5.43.

3.2. Proteolysis and water activity

One of the parameters that characterised the tested cheeses was the content of WSE, whose values are presented in Table 2. The

Table 1
Composition of goat cheeses.[a]

Composition	SHG	HG	EHG
Moisture (g 100 g^{-1})	46.40 ± 0.07^c	37.50 ± 0.36^b	29.84 ± 0.34^a
MFFB (%)	63.7	54.9	46.3
Fat (g 100 g^{-1})	27.20 ± 0.07^a	31.68 ± 0.13^b	35.49 ± 0.09^c
FDM (%)	50.7	50.7	50.6
Protein (g 100 g^{-1})	23.10 ± 0.11^a	26.34 ± 0.05^b	30.25 ± 0.08^c
M:P	2.0	1.4	1.0
F:P	1.2	1.2	1.2
Salt (g 100 g^{-1})	0.80 ± 0.08^a	0.95 ± 0.02^b	1.03 ± 0.07^c
Ash (g 100 g^{-1})	2.21 ± 0.10^a	2.41 ± 0.06^b	2.72 ± 0.07^c
pH	5.14 ± 0.06^b	5.08 ± 0.04^a	5.32 ± 0.09^c

[a] Abbreviations are: SHG, semi-hard goat cheese ($n = 8$); HG, hard goat cheese ($n = 7$); EHG, extra hard goat cheese ($n = 5$); MFFB, moisture on a fat-free basis; FDM, fat in dry matter; M:P, ratio of moisture to protein, calculated using the means of moisture and protein; F:P, ratio of fat to protein (where protein = total nitrogen × 6.38). Values represent mean ± standard deviation; values in the same row followed by a different superscript letter are statistically different ($\alpha = 0.05$).

Table 2
Proteolysis of goat cheeses.[a]

Parameter	SHG	HG	EHG
WSE (% TN)	8.4 ± 0.1[a]	10.2 ± 0.2[b]	17.6 ± 0.2[c]
Free amino groups (mg Leu g^{-1})	3.42 ± 0.03[a]	4.23 ± 0.07[b]	7.24 ± 0.05[c]

[a] Abbreviations are: SHG, semi-hard goat cheese ($n = 8$); HG, hard goat cheese ($n = 7$); EHG, extra hard goat cheese ($n = 5$); WSE, water-soluble extract; TN, total nitrogen. Values represent mean ± standard deviation; values in the same row followed by a different superscript letter are statistically different ($\alpha = 0.05$).

cheese with the highest moisture content (46.40 g 100 g^{-1}) had the least WSE (8.4% TN). The lower the moisture content of the cheeses, the higher the level of WSE. Proteolysis in hard cheese was higher by 20%. In extra-hard cheeses, more than two times the WSE (17.6% TN) and free amino groups (7.24 mg Leu g^{-1}) were determined than in semi-hard cheeses.

The water activity of SHG was greatest among the goats' cheeses tested ($a_w = 0.9088$; SD = 0.0039). The lower the moisture level, the lower the value of a_w; this trend was statistically significant ($P < 0.05$). A high correlation coefficient was found between a_w and moisture content, $r = 0.99$. The water activity in HG amounted to $a_w = 0.8567 \pm 0.0044$; in turn, the cheeses with the lowest moisture content were characterised by an a_w within the range 0.8034–0.8166 (mean $a_w = 0.8084$).

During proteolysis, higher contents of non-protein nitrogen are known to reduce the water activity in cheese, as a result of the larger amounts of bound water (Marcos, Alcalá, León, Fernández-Salguero, & Esteban, 1981). Freitas and Malcata (1996) showed that the salting procedure/ripening time interaction had a statistically significant effect on water activity, so the two factors acting together were responsible for a larger decrease in water activity than if the agents were considered independently. Water in the cheese occurs in three forms: bulk water in the serum channels, entrapped water in close proximity to the casein matrix, or as bound water tightly associated and adsorbed by the caseins (Enab, Hassan, Abd, & El-Gawad, 2012). Due to the cheese composition changing during the process of ageing of long-ripened cheese, methods of determination of water activity are insufficient (Saurel et al., 2004). For this reason, the determinations by the NMR and DSC techniques were carried out.

3.3. Characteristics of water distribution and mobility in cheese based on NMR and DSC

The low-field NMR method allows the values of spin–lattice T_1 and spin–spin T_2 relaxation times to be determined. Molecular studies using the low-field NMR method often allow the analysis of only two water fractions characterised by various possibilities of molecular motion in the system (Anedda, 2015). Values of T_1 reflect the relative bulk water content in relation to bound water, while values of T_2 describe the dynamics of molecules in both the bulk and bound water fractions. In the case of molecular studies, the bulk water fraction is understood as free water with respect to rotational and translational movements. These are water molecules surrounded by other water molecules, and the intermolecular interaction is associated only with the water–water bond. The bound water fraction is made up of hydrogen-bonded or ion-associated water molecules bound to other large molecules of the system, mainly proteins. The molecules of this water fraction are characterised by a limited possibility of rotational movement around their bonds. The translational movement of the molecules of this fraction is also significantly limited. Both values are additionally affected by the presence of fat in the system (Anedda, 2015). Distributed exponential analysis of the NMR T_2 relaxation data revealed the existence of distinctly different water fractions. Values of T_{21}, the so-called short component, describe spin–spin relaxation of the bound water fraction, while values of T_{22} concern spin–spin relaxation of the bulk water fraction (Baranowska, 2011). The results obtained are shown in Table 3.

The spin–lattice relaxation time values decreased with increasing fat and protein content (Table 1). The long component of T_{22} spin–spin relaxation time did not differ between the three types of cheese (SHG, HG, and EHG). It was assumed that the value of this relaxation time can be determined by the mutual ratio of fat to protein (F:P), which was constant and amounted to 1.2. Hence, it can be concluded that the bulk water fraction is mainly a component of water-in-fat emulsions. The short components of T_{21} spin–spin relaxation times were compared with the pH values of the cheeses examined (Fig. 1). The pH increase was manifested by a decrease in the T_{21} value. Thus, the increase in H^+ ion concentration limits the mobility of bound water protons.

For characterisation of the water's state in cheeses, DSC was used, which allows the quantification of the different types of water in the materials by measuring the ice melting/freezing phase transition. DSC enables the determination of the freezable water and unfrozen water, which is the part of the water fraction unable to crystallise because of specific interactions with the proteolipidic cheese matrix.

The results of freezable water content were obtained by the cooling and heating of cheese samples with different contents of moisture (SHG, HG, and EHG). During cooling (results not shown) peaks connected with the liquid–solid exothermic phase transition of fat and water occurred. At a temperature of approximately 15 °C, a first-order transition occurred corresponding to the crystallisation of the triacylglycerols of milk fat. Subsequently, between −24 and −35 °C, there was a very intensive water crystallisation phase transition, seen as a very sharp and narrow peak.

Table 3
The spin–lattice T_1 and short T_{21} and long T_{22} components of spin–spin relaxation times T_2 of goat cheese.[a]

Type of cheese	T_1 (ms)	T_{21} (ms)	T_{22} (ms)
SGH	202.6 ± 0.5	14.7 ± 0.7	48.8 ± 6.3
HG	193.6 ± 0.8	19.4 ± 1.2	45.8 ± 7.1
EHG	126.0 ± 0.4	10.4 ± 1.1	48.5 ± 6.6

[a] Abbreviations are: SHG, semi-hard goat cheese ($n = 8$); HG, hard goat cheese ($n = 7$); EHG, extra hard goat cheese ($n = 5$).

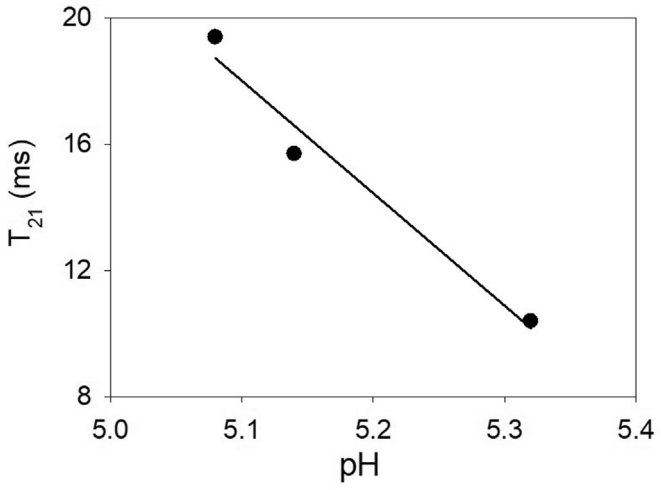

Fig. 1. The relationship between pH of the cheeses and the short components T_{21} of spin–spin T_2 relaxation time.

Formation of ice in cheese occurred at a temperature much lower than 0 °C, which was connected with the phenomenon of supercooling. Similar results for the water crystallisation temperature in emulsions were reported in previous studies (Clausse, 2010; Thanasukarn, Pongsawatmanit, & McClements, 2004). In turn, in the process of heating (Fig. 2) endothermic transitions connected with the solid–liquid phase transition took place. At a temperature between −20 and −6 °C a symmetrical and narrow peak was observed, slightly wider than that of crystallisation, connected with ice melting. Further heating resulted in the appearance of smaller peaks, broader and with a gentle slope, coming from the melting of the triacylglycerols of the milk fat.

In Table 4 the results of the temperature and the enthalpy of ice melting during the heating of cheese samples from −40 °C to 70 °C are shown. It can be seen that for cheese with the highest content of water (SHG), the highest values of temperatures (T_{peak}) and enthalpy ΔH of ice melting were observed. Generally, it can be stated that both the peak temperature and enthalpy progressively decreased with the lowering of moisture. From the values of the ice melting enthalpy, the percentage of freezable water in the water fraction (FW) was calculated according to Eq (3). The lowest value of ice melting enthalpy, noted in EHG, indicated that the greater part of the water, i.e., 79.90% in this cheese, remained unfrozen at a temperature of −40 °C. The DSC cooling and heating curves recorded for SHG, HG, and EHG cheese were very comparable with those obtained by Gliguem et al. (2009), where cheese spreads were analysed. These findings of water behaviour are also consistent with results obtained by NMR, shown in Table 3, where the T_1 parameter was the lowest for the EHG sample, which meant that in this sample the content of bulk water was the lowest. A strong dependence was found between the NMR parameter T_1 and the DSC freezable water content, with a significant correlation coefficient, $r = 0.96$ (Fig. 3).

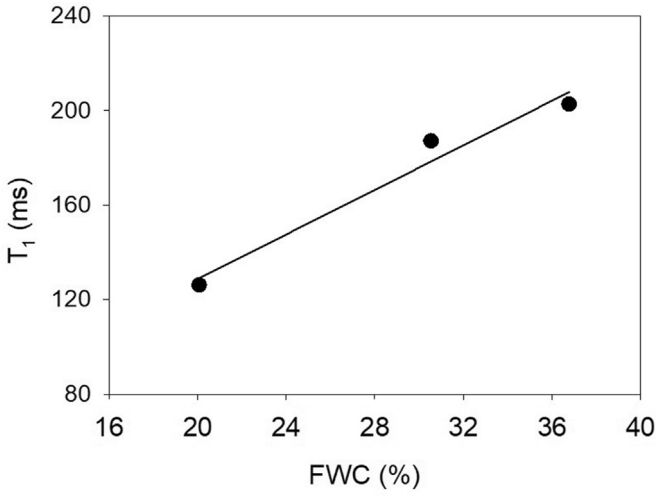

Fig. 3. The relationship between freezable water content (FWC) (Table 3) obtained by DSC analysis and spin–lattice relaxation time (T_1) obtained by NMR technique (Table 4).

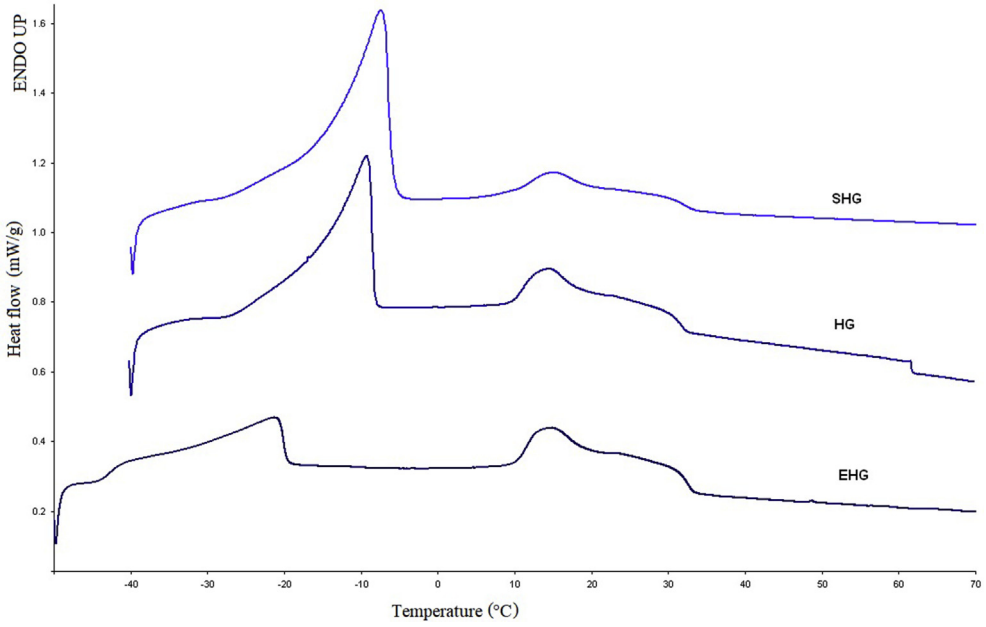

Fig. 2. DSC melting curves of three different types of cheese (SHG-semi hard, HG-hard, EHG-extra hard).

Table 4
DSC characteristics of the phase transition of water in different types of goat cheeses.[a]

Cheese	Temperature, T_{peak} (°C)	Enthalpy of ice melting ΔH (J g^{-1} $_{water}$)	Freezable water content (%)	Unfrozen water content (%)
SHG	−7.12 ± 0.71	122.26 ± 1.57	36.79 ± 0.47	63.21
HG	−9.07 ± 0.84	101.56 ± 2.83	30.56 ± 0.53	69.44
EHG	−19.80 ± 1.47	66.82 ± 3.32	20.10 ± 1.01	79.90

[a] Abbreviations are: SHG, semi-hard goat cheese ($n = 8$); HG, hard goat cheese ($n = 7$); EHG, extra hard goat cheese ($n = 5$). Unfrozen water content values are given by: (100 − freezable water content).

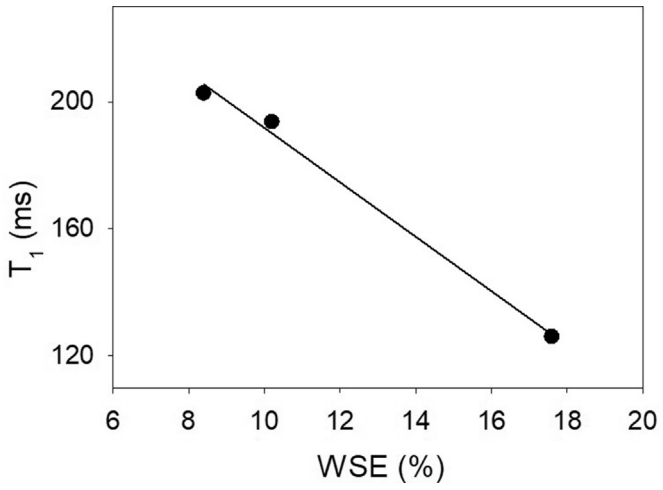

Fig. 4. The relationship between water soluble extract (WSE) (Table 2) and spin–lattice relaxation time T_1 (Table 4).

The increase in the value of spin–lattice relaxation time T_1 means an increase in the proportion of bulk water to bound water. By using the DSC technique, this fact can be seen as an increase in freezable water content (FWC). The obtained relations indicate that freezable water is related to the bulk water fraction in the system. Similar relationships were found between the parameters related to the basic chemical composition of cheese and the molecular properties of water.

The samples of SHG were characterised by the highest moisture content and the lowest protein content. This was manifested by the greatest values of the spin–lattice relaxation time, which indicated that the bulk water fraction was the most common in this system. This suggests that the proteins they act as a factor a strongly binding water in system. A linear dependence was found between the relaxation time values for the spin–lattice (T_1) and WSE (Fig. 4), suggesting that proteolysis has a significant effect on water binding in cheese (expressed by parameter T_1).

4. Conclusions

The behaviour of water in three types of goats' cheese (semi-hard, hard, and extra-hard), differing in water content and with a constant ratio of fat to protein, was investigated. It was observed by NMR and DSC that the lowest content of bulk water was detected in extra-hard cheese (EHG). In this sample, the proportion of bulk water in the total water was the lowest, which indicated that the water was strongly entrapped in the proteolipidic network and bound by the water-soluble substances (WSE) arising after increasing proteolysis. The proteolysis and the presence of water-soluble extracts was a factor influencing the binding of water molecules, causing a decrease in the bulk water content of the system.

Acknowledgements

A part of the study was supported by grant no. 508.784.00/UPP-KJPM from the Polish Ministry of Science and Higher Education.

References

Altan, A., Oztop, M. H., McCarthy, K. L., & McCarthy, M. J. (2011). Monitoring changes in feta cheese during brining by magnetic resonance imaging and NMR relaxometry. *Journal of Food Engineering, 107*, 200–207.

Anedda, R. (2015). Magnetic resonance analysis of dairy processing suitable tools for the dairy industry. In F. Capozzi, L. Laghi, & P. S. Belton (Eds.), *Magnetic resonance in food science. Defining food by magnetic resonance* (pp. 51–64). Cambridge, UK: Royal Society of Chemistry.

AOAC. (1995). *Loss on drying (moisture) in cheese. Method I. Final Action, No. 33.7.03 Official Methods of Analysis of AOAC International* (16th ed.). Arlington, VI, USA: AOAC International.

Arimi, J. M., Duggan, E., O'Sullivan, M., Lyng, J. G., & O'Riordan, E. D. (2008). Effect of refrigerated storage on water mobility and microwave expansion of imitation cheese containing resistant starch. *Journal of Food Engineering, 89*, 258–266.

Baranowska, H. M. (2011). Water molecular properties in forcemeats and finely ground sausages containing plant fat. *Food Biophysics, 6*, 133–137.

Baranowska, H. M., Tomaszewska-Gras, J., Cais-Sokolińska, D., Bierzuńska, P., & Kaczyński, Ł. K. (2017). Water mobility and thermal properties of smoked soft cheese. *Mljekarstvo, 67*, 188–196.

Brosio, E., & Gianferri, R. R. (2009). An analytical tool in foods characterization and traceability. In E. Brosio (Ed.), *Basic NMR in foods characterization* (pp. 9–37). Kerala, India: Research Signpost.

Cais-Sokolińska, D., Bierzuńska, P., Kaczyński, Ł. K., Baranowska, H. M., & Tomaszewska-Gras, J. (2018). Stability of texture, meltability and water mobility model of pizza-style cheeses from goat's milk. *Journal of Food Engineering, 222*, 226–236.

Clausse, D. (2010). Differential thermal analysis, differential scanning calorimetry, and emulsions. *Journal of Thermal Analysis and Calorimetry, 101*, 1071–1077.

Codex. (2013). *Stan 283-1978. Codex general standard for cheese, revision 1999, amendment 2013*. Rome, Italy: WHO/FAO International Food Standards.

Enab, A. K., Hassan, F. A. M., & Abd El-Gawad, M. A. M. (2012). Effect of manufacture steps on cheese structure (review). *International Journal of Academic Research Part A, 4*, 79–89.

Fekadu, B., Soryal, K., Zeng, S., Van Hekken, D., Bah, B., & Villaquiran, M. (2005). Changes in goat milk composition during lactation and their effect on yield and quality of hard and semi-hard cheeses. *Small Ruminant Research, 59*, 55–63.

Folkertsma, B., & Fox, P. F. (1992). Use of the Cd-ninhydrin reagent to assess proteolysis in cheese during ripening. *Journal of Dairy Research, 59*, 217–224.

Fox, P. F. (1989). Proteolysis during cheese manufacture and ripening. *Journal of Dairy Science, 72*, 1379–1400.

Freitas, A. C., & Malcata, F. X. (1996). Influence of milk type, coagulant, salting procedure and ripening time on the final characteristics of Picante cheese. *International Dairy Journal, 6*, 1099–1116.

Gliguem, H., Ghorbel, D., Grabielle-Madelmont, C., Goldschmidt, B., Lesieur, S., Attia, H., et al. (2009). Water behavior in processed cheese spreads. DSC and ESEM study. *Journal of Thermal Analysis and Calorimetry, 98*, 73–82.

Haenlein, G. F. W. (2007). About the evolution of goat and sheep milk production. *Small Ruminant Research, 68*, 3–6.

Kanawjia, S. K., Rajesh, P., Sabikhi, L., & Singh, S. (1995). Flavour, chemical and textural profile changes in accelerated ripened Gouda cheese. *LWT-Food Science and Technology, 28*, 577–583.

Kirmaci, H. A., Hayaloglu, A. A., Özer, H. B., Atasoy, A. F., & Türkoglu, H. (2014). Evolution of proteolysis in Urfa cheese made from ewe's milk by wild type starter culture systems. *Small Ruminant Research, 119*, 120–129.

Kuchroo, C. N., & Fox, P. F. (1982). Soluble nitrogen in Cheddar cheese: Comparison of extraction procedures. *Milchwissenschaft, 37*, 331–334.

Lewicki, P. P. (2004). Water as the determinant of food engineering properties. A review. *Journal of Food Engineering, 61*, 483–495.

Marcos, A., Alcalá, M., León, F., Fernández-Salguero, J., & Esteban, M. A. (1981). Water activity and chemical composition of cheese. *Journal of Dairy Science, 64*, 622–626.

Michaelidou, A., Katsiari, M. C., Voutsinas, L. P., Polychroniadou, A., & Alichanidis, E. (2007). Effect of multiple-species starters on peptide profile and free amino acids in low-fat Kefalograviera-type cheese. *Food Chemistry, 104*, 800–807.

Moschopoulou, E., Anisa, T., Katsaros, G., Taoukis, P., & Moatsou, G. (2010). Application of high-pressure treatment on ovine brined cheese: Effect on composition and microflora throughout ripening. *Innovative Food Science and Emerging Technology, 11*, 543–550.

Noronha, E., Duggan, G. R., Ziegler, E. D., O'Riordan, M., & O'Sullivan, A. (2008a). Inclusion of starch in imitation cheese: Its influence on water mobility and cheese functionality. *Food Hydrocolloids, 22*, 1612–1621.

Noronha, N., O'Riordan, E. D., & O'Sullivan, M. (2008b). Influence of processing parameters on the texture and microstructure of imitation cheese. *European Food Research and Technology, 226*, 385–393.

Pajonk, A., Saurel, R., Andrieu, J., Laurent, P., & Blanc, D. (2003). Heat transfer study and modeling during Emmental ripening. *Journal of Food Engineering, 57*, 249–255.

Poveda, J. M., Sanchez-Palomo, E., Perez-Coello, M. S., & Cabezas, L. (2008). Volatile composition, olfactometry profile and sensory evaluation of semi-hard Spanish goat cheeses. *Dairy Science & Technology, 88*, 355–367.

Requena, T., De la Fuente, M. A., Fernandez de Palencia, P., Juárez, M., & Pelaez, C. (1992). Evaluation of a specified starter for the production of semi-hard milk cheese. *Le Lait, 72*, 437–448.

Ryffel, S., Piccinali, P., & Butikofer, U. (2008). Sensory descriptive analysis and consumer acceptability of selected Swiss goat and sheep cheeses. *Small Ruminant Research, 79*, 80–86.

Saurel, R., Pajonk, A., & Andrieu, J. (2004). Modelling of French Emmental cheese water activity during salting and ripening periods. *Journal of Food Engineering, 63*, 163–170.

Shakeel-Ur Rehman, McSweeney, P. L. H., Banks, J. M., Brechany, E. Y., Muir, D. D., & Fox, P. F. (2000). Ripening of Cheddar cheese made from blends of raw and pasteurised milk. *International Dairy Journal, 10*, 33–44.

Singh, T. K., Fox, P. F., Hojrup, P., & Healy, A. (1994). A scheme for the fractionation of cheese nitrogen and identification of principal peptides. *International Dairy Journal, 4*, 111–122.

Thanasukarn, P., Pongsawatmanit, R., & McClements, D. J. (2004). Impact of fat and water crystallization on the stability of hydrogenated palm oil-in-water emulsions stabilized by whey protein isolate. *Colloids and Surfaces A: Physicochemical and Engineering Aspects, 246*, 49–59.

Wang, H., & Sun, D. (2002). Melting characteristics of cheese: Analysis of effect of cheese dimensions using computer vision techniques. *Journal of Food Engineering, 52*, 279–284.

Węglarz, W. P., & Harańczyk, H. (2000). Two-dimensional analysis of the nuclear relaxation function in the time domain: The program CracSpin. *Journal of Physics D: Applied Physics, 33*, 1909–1920.